An arrangement for irradiating cultured mammalian cells with aluminium characteristic ultrasoft X-rays

1987 Phys. Med. Biol. 32 1615

(http://iopscience.iop.org/0031-9155/32/12/009)

Phys. Med. Biol., 1987, Vol. 32, No 12, 1615–1626. Printed in the UK

An arrangement for irradiating cultured mammalian cells with aluminium characteristic ultrasoft x-rays

M Folkard, B Vojnovic, K M Prise and B D Michael

Cancer Research Campaign Gray Laboratory, Mount Vernon Hospital, Northwood, Middlesex, HA6 2RN, UK

Received 16 June 1987

Abstract. Ultrasoft x-rays are useful for testing the validity of mechanistic models of biological damage caused by radiation. Described here is the construction and operation of a cold-cathode transmission-target discharge tube for irradiating mammalian cells *in vitro* with aluminium characteristic x-rays (1.487 keV). Particular attention is given to the problems of sample preparation and dosimetry for this shallowly penetrating radiation. The proportion of contaminating bremsstrahlung radiation is measured to establish the optimum operating conditions. Preliminary data from experiments using V79 Chinese hamster cells show that aluminium characteristic x-rays are about twice as effective at inactivating the cells as 250 kV_p x-rays.

1. Introduction

The special properties of ultrasoft x-rays (x-rays with energies below 5 keV) continue to be useful for testing the validity of models that attempt to explain certain mechanisms of biological radiation damage. The dual-action model (Kellerer and Rossi 1972, 1978) suggests interaction distances up to approximately 10 μm. However, data from experiments using ultrasoft x-rays show that interactions over distances greater than 10 nm are not required for efficient cell killing (Goodhead *et al* 1979). Ultrasoft x-rays interact with matter almost entirely by the photoelectric effect, producing electrons that deposit their energy in small, localised volumes. For example, aluminium characteristic K x-rays (1.487 keV) produce electrons with a range of about 0.07 μm. It is this property that makes ultrasoft x-rays particularly useful for testing models involving specific interaction distances.

There are several methods by which ultrasoft x-rays can be generated; for instance, by using a hot-cathode arrangement as in conventional x-rays, or by producing characteristic radiation by proton bombardment (Bernstein and Lewis 1954, Goodhead and Bance 1984). The simplest approach, however, is to excite characteristic radiation by maintaining a low-pressure discharge of a few mA between a cold cathode and a suitable target. If the target is fabricated from thin foil, then it can also serve as a transmission window for the radiation. The technique of generating characteristic radiation by this method was first described by Lea (1941). More recent sources, such as that used by Neary *et al* (1964) and later by Goodhead and Thacker (1977) and described by Hoshi *et al* (1985) are essentially based upon Lea's design. Described in this paper is the design, construction and operation of a cold-cathode transmission-target discharge tube for irradiating mammalian cells *in vitro*. The discharge tube described here is based upon this proven design, however operation of the source has

0031-9155/87/121615+12$02.50

been greatly simplified by incorporating a feedback arrangement to stabilise the discharge. This, together with electronic control of dose delivery enables the production of exactly reproducible exposures. Preliminary results are presented showing the survival of V79 Chinese hamster cells after exposure to aluminium characteristic x-rays and 250 kV_p x-rays.

Severe constraints are placed upon the geometry for sample irradiations because of the considerable attenuation that this type of radiation experiences in matter. For example, for aluminium K x-rays, the intensity is reduced to one half of its incident value in only 4.9 μm of water, or 4.5 mm of air. Difficulties also arise when attempting to quantify the beam dosimetrically. Described here are the methods of sample preparation and support, and the use of a thin-window extrapolation-type ionisation chamber for making dosimetry measurements of this radiation source.

A disadvantage of the cold-cathode discharge tube, compared with the method of proton bombardment, is that significant bremsstrahlung radiation can be produced. A portion of this radiation will have an energy greater than the characteristic radiation and is therefore considerably more penetrating. It is important that this does not represent a significant portion of the total dose if the special properties of ultrasoft x-rays are not to be diluted out. It is shown here that for 2.6 keV bombarding electrons the bremsstrahlung radiation contributes no more than 0.2% of the total surface dose.

2. Method

2.1. Construction of the source

The construction of the discharge tube is illustrated in figure 1. In operation, a discharge of a few mA at 2–5 kV is maintained between an aluminium concave cathode, supported

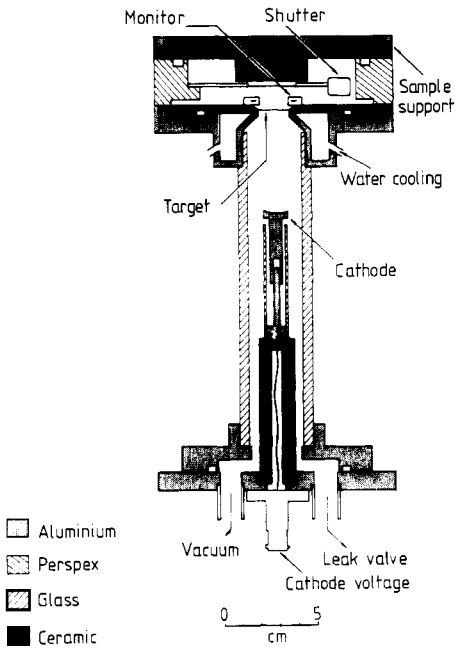

Figure 1. Construction of the discharge tube.

by an insulating ceramic pillar, and a 2.7 mg cm^{-2} (10 μm) thick, 16 mm diameter aluminium foil anode. The bombarding electrons are stopped by the foil, producing aluminium characteristic K x-rays. The tube is pumped continuously and a pressure of 0.1–1.0 mbar is maintained within the tube by a remotely controlled leak valve (manufactured by Vacuum Generators, model MD6). A Pirani gauge is used to monitor the pressure. The foil anode also serves as a vacuum window through which the aluminium characteristic x-rays are transmitted. The foil is supported by a 0.5 mm thick aluminium plate, into which a 'honeycomb' of 1 mm diameter holes has been drilled. The transmission coefficient of the plate is approximately 50%. Water may be pumped through a cavity in the anode assembly so that the target can be cooled if necessary.

To monitor the radiation, a narrow-section ring ionisation chamber is installed 4 mm in front of the target, and it defines an aperture 17 mm in diameter. The chamber comprises a 24 mm diameter annular collecting electrode, enclosed on three sides by a brass polarising electrode. The fourth side is constructed from 2.7 mg cm^{-2} thick aluminium foil, through which the ultrasoft x-rays are admitted to the chamber. A polarising voltage of +150 V is normally used. It is important that the charge-collecting volume is enclosed in this way, otherwise the close proximity of the extrapolation chamber or the sample support will distort the electric field of the monitor chamber in an unpredictable way.

During an experiment, the source remains energised and an externally mounted leaf shutter (manufactured by Vincent Associates Inc.) located 12.5 mm from the target is used to start and stop the sample irradiations. This shutter was designed for optical work but can be successfully employed in this experiment because of the limited beam penetration. By using an external shutter, the stability of the discharge is not affected by the action of this assembly. The leaf shutter is supported above the target and the monitor by a perspex annulus that forms an O-ring seal with the top of the source. A similar seal is made above the shutter with the sample support so that the cells are irradiated in an enclosed volume. By flushing gas through the volume it is possible to irradiate the cells under oxic or hypoxic conditions. This will, of course, affect the sensitivity of the monitor chamber and also the degree of attenuation experienced by the photons between the anode and the sample.

2.2. Control electronics

The electronic control unit for the x-ray source is illustrated in figure 2 and consists of two distinct sections, one controlling the operation of the source and the other monitoring the dose delivered by the source. The source is powered by a 25 W, 5 kV, 5 mA EHT power supply (Brandenburg Ltd type 732N), although typically a lower power is used (5–15 W). The complete control unit along with a Pirani vacuum gauge is housed in a 5.25 in × 19 in (1 in ≈ 2.54 cm) wide rack. The operator has control and digital readout of the tube current and voltage, analogue readout of the dose rate (as measured by the ring monitor chamber) and can present and read the required dose counts. Start, stop and reset push-buttons control the leaf shutter and the dose-monitor batch counter. The shutter closes when the stop button is pressed or when the batch counter reaches the preset number of counts.

The dose delivered is determined by integrating the current from the ring chamber. The current is first converted to a voltage (Analogue Devices 310J electrometer, arranged as a current to voltage converter, 1 nA and 10 nA FSD) and then to frequency

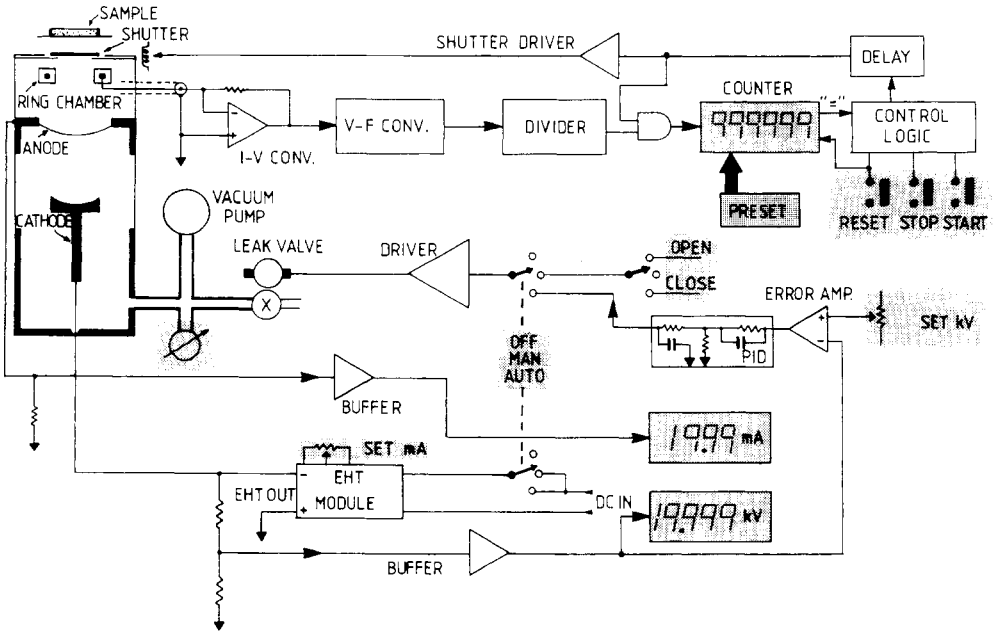

Figure 2. Arrangement for controlling the operation of the source and monitoring the delivered dose.

(100 kHz FSD). The resulting output pulse train is divided down to approximately 100 Hz and applied to a six-decade batch counter. The number stored in the counter is thus proportional to the integral of the chamber current. When the required count has been reached a control logic circuit is triggered which closes the exposure shutter and, after a time delay of 2 ms (to match the closing time of the shutter), disables any further counts to the batch counter. This is necessary as the ring chamber continues to monitor the beam even with the shutter closed.

The discharge tube is operated in the constant-current mode; the output compliance of the EHT module used is more than adequate for this purpose and the tube current can be varied over the range 0–5 mA using a ten-turn potentiometer. The discharge tube anode is isolated form the ground to enable a 100 Ω current-sensing resistor to be introduced. The voltage developed across this resistor is amplified and a 3.5 digit voltmeter is used to display the tube current (19.99 mA FSD). The tube voltage is monitored with a 1000:1 voltage divider network and displayed on a 4.5 digit voltmeter (19.999 kV FSD). The tube voltage is used as a feedback signal in a control loop which stabilises the operating voltage by adjusting the pressure within the tube. A small DC motor attached to the leak valve is energised by the error signal of a feedback control loop, generated by comparing the tube voltage with a preset value determined by the position of a ten-turn potentiometer, which is in the range 0–5 kV. For good stability against load and set-point changes it is necessary to use a high proportional loop gain; unfortunately, when using a simple proportional control this must be restricted because of the unavoidable lag introduced by the leak-valve/motor assembly. Nevertheless, a proportional-integral-derivative type of control loop can be readily optimised to provide a critically damped response over a restricted range of set-point voltages. In our case we were able to obtain a risetime (10–90%) for the tube voltage of 2.5 s over the range 1–3 kV in response to a 500 V set-point change; this results in a settling time

(to within 0.5% of the required value) of 30 s. Similar settling times are obtained for a load current change of 0.5 mA. This level of performance was felt to be more than adequate and can be readily obtained with a little patience by optimising the loop parameters. It was decided to stabilise the tube voltage rather than the x-ray monitor output because the monitor sensitivity is dependent on the tube voltage (see § 3). Two small toggle switches, interlocked to the EHT supply, can be used to adjust the leak valve manually. These are used when the tube is energised initially to obtain approximately the required operating conditions before switching to automatic control.

2.3. Sample preparation

So far, all the experiments have been undertaken using V79-379A Chinese hamster cells obtained from a cell line maintained at this laboratory for some years. The cells are grown in a suspension of Eagle's minimal essential medium, supplemented with 7.5% foetal calf serum, at 37° C in 95% air and 5% CO_2. They are irradiated as a monolayer on the surface of a 13 mm diameter Durapore polyvinylidene difluoride hydrophilic filter (Millipore Corporation) with a 0.22 μm pore size. The samples are prepared by placing the filters on 1% agar in the above medium, set in Petri dishes. The cells are concentrated to approximately 2×10^7 cells/ml of medium. A 20 μl sample is placed on each filter and is left for 15 min to allow the medium to soak through. It has been found that these particular filters have a number of advantages in this application. Firstly, being hydrophilic, the filters remain moist without an appreciable film of water lying over the surface of the cells (which would attenuate the ultrasoft x-rays by an indeterminate amount). Secondly, the filter material inhibits the cells from attaching readily to the surface, so that they do not 'flatten out' and are easily removed after irradiation.

To irradiate the cells, the filters are removed from the agar and attached to an aluminium platter by surface tension. The platter is simply a flat plate that holds the sample 16.8 mm from the target with a small thermoelectric cooling device on the reverse side used in order to cool the platter by a few °C to prevent the filter from drying out. After irradiation, the cells are washed from the filter and diluted to give 100–200 viable cells per plate. The reulting cell colonies can be counted one week later.

2.4. Dosimetry

An extrapolation-type ionisation chamber, designed and constructed at this laboratory, is used to calibrate the monitor chamber. The extrapolation chamber consists of two parallel-plate electrodes, the separation of which can be precisely controlled. The lower polarising electrode (through which the radiation is admitted) is a 20 mm diameter, lightly aluminised, 0.332 mg cm^{-2} thick Mylar window maintained at +240 V. The upper collecting electrode is a 13 mm diameter copper plate, surrounded by a 37 mm diameter guard ring, with a 20 μm insulating gap. The collecting electrode and guard ring form one end of a 38 mm diameter precision threaded cylinder of 1 mm pitch that engages into the body of the chamber. By turning this cylinder, the plate separation can be adjusted with a precision of ±5 μm down to a gap of 0.3 mm. Absolute calibration of the plate spacing has been determined to an accuracy of ±20 μm by measuring the chamber capacitance as a function of plate separation with a Wayne Kerr bridge (model B605). Capacitance measurements were also used to ascertain the

effective charge-collecting area of the plate, giving an area of 136 mm^2, and to check that there was negligible electrostatic deformation of the window.

To calibrate the monitor chamber, the chamber is positioned over the target so that the sample plane is midway between the two electrodes. Accurate location of the chamber is facilitated by three micro-adjustable feet. Ionisation currents are measured using a Keithley 616 electrometer at several collecting volumes. For each measurement, the chamber position is adjusted so that the sample plane remains in the centre of the ionisation cavity. These measurements are used to ascertain the limiting ionisation current per unit plate separation, dI/dx, for an infinitesimally small charge-collecting volume. For measurements with plate spacings between 0.3 and 1.2 mm no departure from linearity was observed. The dose rate, dD/dt, can be calculated using the following expression.

$$\frac{dD}{dt} = \frac{W}{eA\rho} \frac{(\mu/\rho)_s}{(\mu/\rho)_a} k_{tp}\, k_w k_c \frac{dI}{dx} \tag{1}$$

where W is the average energy per ion pair in air for 1.487 keV photons, e is the electronic charge, A is the effective area of the collecting electrode and ρ is the density of air at STP. The parameters $(\mu/\rho)_s$ and $(\mu/\rho)_a$ are the mass attenuation coefficients for the sample and air respectively, k_{tp} is a temperature and pressure correction factor from ambient conditions to STP and k_w is a correction for the attenuation by the chamber window. The factor k_c is a correction for the attenuation of the radiation within the cell itself.

The value used for W is 35 eV per ion pair. This was estimated by Hoshi *et al* (1985) from measurements of the W value for electrons in air (Combecher 1980). Previously, Goodhead and Thacker (1977) obtained the same result by calculating W for air from known W values for propane and methane. The mass attenuation coefficients for air and for the sample were calculated from the tabulations of Henke *et al* (1982). The calculated value for air is 1224 $cm^2\,g^{-1}$. The value chosen for $(\mu/\rho)_s$ will depend upon the assumptions made about the chemical composition of the sample. It is important to realise that the attenuation coefficient for this type of radiation is strongly dependent upon the absorber atomic number. The compositions of several tissue types were obtained from table 7 of Seltzer and Berger (1982) and from ICRP (1975), and the attenuation coefficients for muscle, blood, brain and spleen have been calculated as 1307, 1335, 1303 and 1319 $cm^2\,g^{-1}$ respectively. It is not known which of these tissue types best represents the mammalian cells used in these experiments, so the mean value for the four tissue types mentioned above is used for $(\mu/\rho)_s$ (1316 $cm^2\,g^{-1}$). The correction factor k_w has the value 1.486, which has been deduced from attenuation measurements of the chamber window material.

To estimate the effect of the attenuation of x-rays within the cell requires knowledge of the size, shape and density of the cell, as well as the location of the radiobiologically 'sensitive region' for radiation damage within the cell. Assumptions made about the cellular dimensions are based on the structure proposed by Datta *et al* (1976) for Chinese hamster ovary cells freshly plated onto membrane filters. They depict the cell as a flattened sphere, 18 μm wide and 10 μm high. The nucleus is supported roughly centrally, with a width of 15 μm and a height of 8 μm. This cell structure has been modelled mathematically so that the dose at any point within the cell, relative to the surface dose, can be computed. By averaging the relative dose over the radiation-sensitive region of the cell, an estimate of k_c is obtained. The work of Datta *et al* and, later, that of Cole *et al* (1980) attribute cell inactivation by radiation to DNA damage

at the surface of the nucleus. If this model for the sensitive region is used, then $k_c = 0.64$. If it is assumed that the whole of the nucleus constitutes the sensitive region, then $k_c = 0.56$.

3. Results

As mentioned in § 1, the purity of the characteristic radiation should not be degraded significantly by the accompanying bremsstrahlung radiation. It is expected that the bremsstrahlung radiation energy spectrum will be a continuum that extends as high as the bombarding electron energy, with an intensity which is a strong function of the source voltage. Thus increasing the voltage will have the undesirable effect of producing contaminating radiation that is both more intense and more penetrating.

To ascertain the purity of the radiation from the source, absorption measurements were made at several voltages. The results are shown in figure 3. Three voltages were investigated, 2610, 3010 and 3510 V, and these are represented by diamond, circle and square symbols respectively. The curves illustrate how the penetration of the radiation is affected by successive layers of 0.332 mg cm^{-2} thick Mylar film. The full line is extrapolated from the data for attenuation factors less than 10 and represents the expected attenuation of the characteristic radiation. The closed symbols are estimates of the bremsstrahlung radiation, obtained by subtracting the full line from the absorption data (open symbols). The contribution of bremsstrahlung radiation has been estimated by assuming that the radiation is absorbed exponentially and by fitting the appropriate function (shown as broken lines in figure 3). Although this is an approximation (because the bremsstrahlung radiation is not monoenergetic), it is nevertheless adequate for our estimates. Thus it can be concluded that the bremsstrahlung radiation contributes approximately 0.2, 0.5 and 1.8% of the total dose at the cell surface for source voltages of 2610, 3010 and 3510 V respectively.

The mean dose rate to the cell-sensitive site as a function of the source voltage is shown by the open symbols in figure 4. The closed symbols show the contribution

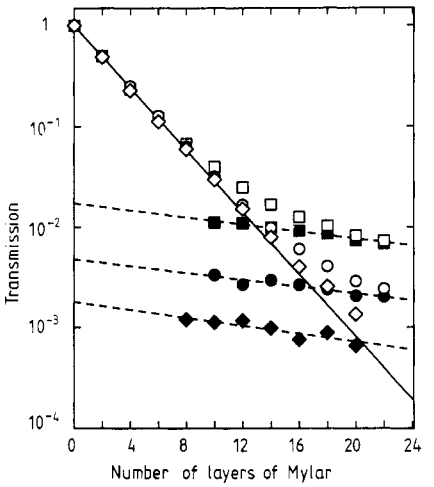

Figure 3. Attenuation of the radiation beam by successive layers of 0.332 mg cm^{-2} thick Mylar film at three voltages: 2610 kV, ◇; 3010 kV, ○; and 3510 kV, □. The corresponding closed symbols represent the contributions from bremsstrahlung radiation obtained by subtracting the full line from the values represented by the open symbols.

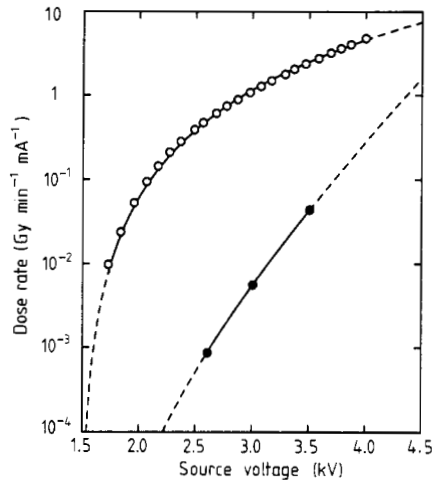

Figure 4. ○, the dose rate at the sample position as a function of voltage. The fitted curve to these data is $dD/dt = 0.373(V - 1.487)^{2.71}$. ●, the contribution from bremsstrahlung radiation.

from bremsstrahlung radiation. It can be clearly seen that there is a rapid increase in the dose rate as the source voltage is raised. The full curve through the open symbols is a fitted function of the form $dD/dt = a(V - K)^b$, where V is the source voltage, K is the threshold energy for the production of characteristic x-rays (1.487 keV) and a and b are the fitted parameters. Thus a wide range of dose rates is available by changing the source voltage, bearing in mind the limitation imposed by the decreased purity of the beam at higher voltages. In practice, the voltage is kept below 3000 V to keep the contribution from bremsstrahlung radiation below 0.5%.

When setting the voltage, it should be realised that the monitor chamber calibration factor (i.e. the integrated charge from the monitor per Gy of radiation to the sample) is only valid for the source operating conditions at which the chamber was calibrated. This is apparent from the results shown in figure 5. This graph illustrates how the

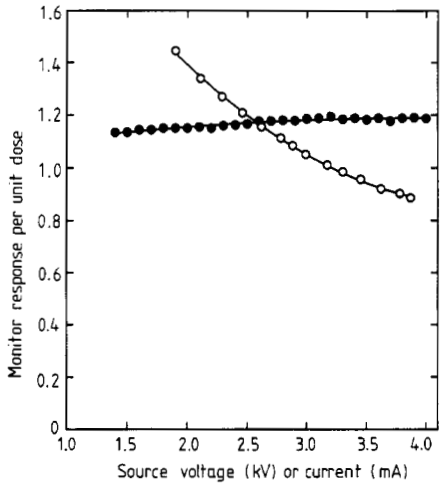

Figure 5. Variation in the dose monitor response with source voltage, ○, and current, ●.

number of monitor divisions (monitor divisions are arbitrary units proportional to the integrated current) per Gy of radiation is affected by variations in the source voltage and current. The open symbols show how the chamber calibration factor varies with voltage, while maintaining a constant current of 2.2 mA. The closed symbols show how the calibration varies with discharge current for a fixed voltage of 2600 V. It is apparent that the chamber calibration is more sensitive to changes in the source voltage than it is to current variations. It is not clear why this dependence on source voltage exists; it may be due to changes in the physical characteristics of the discharge, such that there is a higher radiation output from the centre of the target (relative to the edge) as the voltage is increased. Clearly, it is important that the control electronics reliably stabilise the source at the predetermined voltage and current settings during an experiment. The long-term variation of the voltage has been measured as less than ±5 V (i.e. 0.38% at 2.6 kV), which represents a change in the calibration factor of the monitor chamber of only 0.27%. The long-term current stability is better than 0.3%, which is not significant considering the lesser dependence of the monitor calibration on current (the calibration factor changes by only 3% between 2 and 4 mA). Should it be necessary to alter the dose rate during an experiment then the data of figure 5 can be used to adjust the calibration factor accordingly. Measurements have been made of the change in sensitivity of the (unsealed) monitor chamber caused by flushing gas through the sample cavity. Variations due to temperature and pressure changes with a low flow rate of air are small (below 1%). For other gas mixtures however, the chamber sensitivity changes due to the different W value and attenuation coefficient of the gas. This must be accounted for in the dosimetry since the chamber is calibrated in air.

Using the filter arrangement described in § 2.3, Chinese hamster V79-379A fibroblasts were exposed to aluminium characteristic ultrasoft x-rays in air at a dose rate of 2.2 Gy min^{-1}; the surviving fraction of cells is plotted against dose in figure 6. A shouldered cell survival curve was fitted, for doses of 0–6 Gy, with a linear quadratic function of the form

$$\text{surviving fraction} = e^{-(\alpha D+\beta D^2)} \tag{2}$$

where α and β are constants. The error bars are plus or minus one standard error of the mean. At doses greater than 8 Gy there is an indication of a tail region on the cell survival curves. The dose received by the cells was calculated using the assumptions described in § 2.4 with the nuclear membrane being considered the radiation-sensitive region. The data shown are from three separate experiments and are plotted alongside cell survival data from V79 cells in suspension irradiated with 250 kV_p x-rays at a dose rate of 1.8 Gy min^{-1}. The relative biological effectiveness (RBE) of aluminium characteristic ultrasoft K x-rays in comparison to 250 kV_p x-rays is 2.1 at a surviving fraction of 0.01.

4. Discussion

Throughout its use, the source has been observed to give precisely reproducible exposures. The long-term stability of the radiation output has been measured as better than 3% at 2.6 kV, 3 mA over a period of 4 h of continuous operation. The monitor chamber calibration factor at these settings has fluctuated by less than ±3% over a period of four months (after temperature and pressure corrections).

Several factors contribute to the uncertainties in the absorbed dose at the sensitive site. The uncertainty in the W value for air is about 2%. This is the experimental error quoted by Combecher (1980) for the electron W-value measurements used to derive this parameter. The uncertainty in the mass attenuation coefficient is due to an imprecise knowledge of the cell composition and has been estimated to be about 2-3%. The close proximity of the sample to the target means that there is inevitably a significant dose variation across the sample region. Detailed calculations show that the dose to the edge of the sample is between 8 and 12% lower than the dose to the centre. These values represent the two extreme situations where the radiation output from the target is assumed to be uniform, or where the x-rays are produced only at the centre of the target. Probably the greatest source of error is in estimating the radiation attenuation within the sample. First, the assumption that there is only a negligible layer of medium covering the cell may not be correct. For every 1 μm of medium over the cell, the x-rays are attenuated by 13%. Second, it is not clear how well the proposed cell structure represents the experimental situation. Assuming that the nuclear membrane is the sensitive site, then a variation of ±10% in the thickness of the cytoplasmic layer surrounding the nucleus causes a ±9% change in k_c. Note that this rapid attenuation with thickness means there is a considerable spread in the amount of dose absorbed within different parts of the cell. The calculated dose to the sensitive region varies between 0.28-0.87 of the dose at the cell surface. Furthermore, a detailed analysis of how the absorbed dose varies within the sensitive region of the cell shows that a large percentage of the nuclear membrane receives a dose that is close to the upper and lower extremities of this dose variation, so that only a relatively small fraction receives a dose near to the mean value.

As the data in figure 6 show, the source has been used successfully to irradiate mammalian cells grown in culture. Quantitatively similar results have been obtained

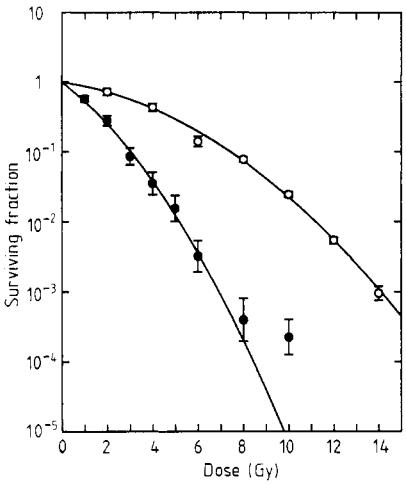

Figure 6. Cell survival of V79 cells irradiated in air with 1.487 keV x-rays, ●, at a dose rate of 2.2 Gy min^{-1}, or with 250 kV_p x-rays, ○, at a dose rate of 1.8 Gy min^{-1}. The surviving fraction of cells is plotted against the mean dose received by the cells assuming the nuclear membrane to be the sensitive site. The error bars are ±one standard error of the mean. The data are fitted with a linear quadratic function where for 1.487 keV x-rays, $\alpha = 0.567\ Gy^{-1}$ and $\beta = 6.21 \times 10^{-2}\ Gy^{-2}$ and for 250 kV_p x-rays, $\alpha = 0.109\ Gy^{-1}$ and $\beta = 2.7 \times 10^{-2}\ Gy^{-2}$.

in comparison with the work of Cox *et al* (1977) using V79 cells, with aluminium characteristic ultrasoft K x-rays being approximately twice as effective at cell inactivation as 250 kV_p x-rays. The use of Durapore filters for collection and irradiation provides a useful means of studying cells grown in suspension. Previous studies with mammalian cells have used attached cells grown in monolayer on melinex dishes (Goodhead and Thacker 1977), although a filter arrangement has been used for irradiation of yeast (Frankenberg *et al* 1986). The suggestion of a tail at higher doses may be due to shielding of some of the cells, either by the medium or by other cells.

Acknowledgments

The authors wish to thank B H Bloomfield and D W Nash of the Gray Laboratory workshop for the mechanical construction of the source and R G Newman for construction of the source controller. Thanks are due to S Davies for her help with the preparation and irradiation of the cells. The authors wish to acknowledge the financial support of the Cancer Research Campaign.

Résumé

Dispositif permettant l'irradiation des cellules de mammifères en culture avec les rayons X caractéristiques de l'aluminium de très basse énergie.

Les rayons X de très basse énergie sont utiles pour étudier la validité des modèles décrivant les mécanismes des effets biologiques des rayonnements. Ce travail décrit la construction et la mise en oeuvre d'un tube à décharge, à cathode froide et anode à transmission, pour l'irradiation de cellules de mammifères *in vitro*, avec les rayons X caractéristiques de l'aluminium (1,487 keV). Les auteurs apportent une attention particulière aux problèmes de préparation des échantillons et à la dosimétrie pour ce rayonnement à faible pénétration. La contamination par le rayonnement de freinage a été déterminée de manière à définir les conditions opératoires optimales. Des données préliminaires à partir d'études utilisant des cellules de hamster chinois V79 montrent que les rayons X caractéristiques de l'aluminium sont environ deux fois plus efficaces que les rayons X de 250 kV_p pour l'inactivation des cellules.

Zusammenfassung

Eine Anordnung zur Bestrahlung von Säugetierzellkulturen mit ultraweichen charakteristischen (Aluminium) Röntgenstrahlen.

Ultraweiche Röntgenstrahlen sind nützlich zur Überprüfung der Gültigkeit mechanistischer Modelle biologischer Strahlenschäden. In der vorliegenden Arbeit werden Konstruktion und Betriebsweise einer Transmissionsentladungsröhre mit kalter Kathode zur Bestrahlung von Säugetierzellen *in vitro* mit charakteristischen (Aluminium) Röntgenstrahlen (1.487 keV) beschrieben. Dabei werden insbesondere die Probleme der Probenaufbereitung und der Dosimetrie für diese wenig durchdringende Strahlung berücksichtigt. Der Anteil kontaminierender Bremsstrahlung wurde gemessen, um so die optimalen Betriebsbedingungen zu gewährleisten. Vorläufige experimentelle Ergebnisse mit Hilfe von chinesischen V79-Hamsterzellen zeigen, daß charakteristische (Aluminium) Röntgenstrahlen doppelt so wirksam sind bei der Zellinaktivierung wie 250 kV_p-Röntgenstrahlen.

References

Bernstein E M and Lewis H W 1954 *Phys. Rev.* **95** 83

Cole A, Meyn R E, Chen R, Corry P M and Hittelman W 1980 *Radiation Biology in Cancer Research* ed R E Meyn and H R Withers (New York: Raven) p 33

Combecher D 1980 *Radiat. Res.* **84** 189

Cox R, Thacker J and Goodhead D T 1977 *Int. J. Radiat. Biol.* **31** 561

Datta R, Cole A and Robinson S 1976 *Radiat. Res.* **65** 139
Frankenberg D T, Goodhead D T, Frankenberg-Schwager M, Harbich R, Bance D A and Wilkinson R E 1986 *Int. J. Radiat. Biol.* **50** 727
Goodhead D T and Bance D A 1984 *Phys. Med. Biol.* **29** 535
Goodhead D T and Thacker J 1977 *Int. J. Radiat. Biol.* **31** 541
Goodhead D T, Thacker J and Cox R 1979 *Int. J. Radiat. Biol.* **36** 101
Henke B L, Lee P, Tanaka T J, Shimabukuro R L and Fujikawa B K 1982 *At. Data Nucl. Data Tables* **27** 1
Hoshi M, Goodhead D T, Brenner D J, Bance D A, Chmielewski J J, Paciotti M A and Bradbury J N 1985 *Phys. Med. Biol.* **30** 1029
ICRP 1975 *Reference Man: Anatomical, Physiological and Metabolic Characteristics, Publication 23* (Oxford: Pergamon)
Kellerer A M and Rossi H H 1972 *Current Topics Radiat. Res.* **8** 85
—— 1978 *Radiat. Res.* **75** 471
Lea D E 1941 *Am J. Roentgenol.* **45** 614
Neary G J, Savage J R K and Evans H J 1964 *Int. J. Radiat. Biol.* **8** 1
Seltzer S M and Berger M J 1982 *Int. J. Appl. Radiat. Isot.* **33** 1189